

H₂ Binding to and Fluxional Behavior of Ir(H)₂X(P^tBu₂R)₂ (X = Cl, Br, I; R = Me, Ph)

Bryan E. Hauger, Dmitry Gusev,* and Kenneth G. Caulton*

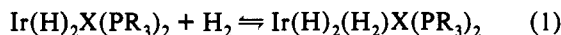
Contribution from the Department of Chemistry, Indiana University, Bloomington, Indiana 47405

Received July 12, 1993*

Abstract: The molecules Ir(H)₂X(P^tBu₂Ph)₂ (X = Cl, Br, I) all show low-temperature ¹H NMR spectra consistent with a structure with inequivalent hydrides, one of which is *trans* to X and one *trans* to an empty coordination site. T₁ measurements suggest that all three molecules have very similar hydride/hydride distances. Hydride rearrangement ΔH[‡] values show little dependence on the halide identity. The decoalescence behavior is not observed for the analogous compounds with P^tBu₂Me. While P^tBu₂Ph compounds show only T₁ and spin-saturation transfer evidence for H₂ binding, the P^tBu₂Me compounds show (at low temperature) signals for both H₂ adduct and five-coordinate species. Line shape analysis of the variable-temperature ³¹P{¹H} NMR spectra permits the determination of ΔH[‡], ΔS[‡], ΔH[°], and ΔS[°] for H₂ dissociation. These parameters have been determined for Cl, Br, and I and (for the chloride case) when deuterium replaces all hydrogens on Ir. The transition state for H₂ dissociation is "tight" (based on ΔS[‡]) and it is enthalpically most accessible for the best π-donor halide, Cl. This same effect stabilizes the five-coordinate species most for chloride, and thus makes the activation enthalpy largest for H₂ binding. The ΔH[°] values for H₂ dissociation increase down the halogen group.

Introduction

A detailed study of the reactions between the formally unsaturated Ir(H)₂X(PR₃)₂ and H₂ is interesting for several reasons. Many η²-H₂ complexes have been synthesized for their theoretical significance and potential importance in catalysis.¹ However, few systems are amenable to kinetic analysis of η²-H₂ complex formation (or destruction). M(H₂)(CO)₃(PCy₃)₂ (M = Cr, W) is the only system to date for which both kinetic and thermodynamic parameters of H₂ binding have been determined.² The formation of Ir(H)₂(H₂)Cl(PR₃)₂ (R = Prⁱ, Cy, ^tBu) from Ir(H)₂Cl(PR₃)₂ and H₂ (eq 1) was initially described by Jensen



*et al.*³ We also observed this reaction as a part of complex transformations of IrHCl₂(PR₃)₂ (R = Prⁱ, Cy) under hydrogen in solution.^{4,5} A detailed understanding of the thermodynamics and kinetics of equilibrium 1 would provide a unique opportunity for a meaningful discussion of the effect of halide identity on the stability of both the unsaturated complex, Ir(H)₂X(PR₃)₂, and the 18e Ir(H)₂(H₂)X(PR₃)₂. We report here such a study.

A recent neutron diffraction study of Ir(H)₂Cl(P^tBu₂Ph)₂ revealed that the hydride ligands were crystallographically distinct.⁵ Previous reports^{3,6,7} of proton NMR spectra of molecules of this type have shown only equivalent hydrides. This raises the possibility of different structures in the solid state and in solution.

* Abstract published in *Advance ACS Abstracts*, December 1, 1993.

(1) Jessop, P. G.; Morris, R. H. *Coord. Chem. Rev.* **1992**, *121*, 155. Heinekey, D. M.; Oldham, W. J. *Chem. Rev.* **1993**, *93*, 913.

(2) (a) Gonzalez, A. A.; Hoff, C. D. *Inorg. Chem.* **1989**, *28*, 4295. (b) Millar, J. M.; Kastrop, R. V.; Melchior, M. T.; Horvath, I. T.; Hoff, C. D.; Crabtree, R. H. *J. Am. Chem. Soc.* **1990**, *112*, 9643. (c) Zhang, K.; Gonzalez, A. A.; Hoff, C. B. *J. Am. Chem. Soc.* **1989**, *111*, 3627.

(3) (a) Mediati, M.; Tachibana, G. N.; Jensen, C. M. *Inorg. Chem.* **1990**, *29*, 3. (b) Mediati, M.; Tachibana, G. N.; Jensen, C. M. *Inorg. Chem.* **1992**, *31*, 1827.

(4) Gusev, D. G.; Bakmutov, V. I.; Grushin, V. V.; Vol'pin, M. E. *Inorg. Chim. Acta* **1990**, *177*, 115.

(5) Albinati, A.; Bakmutov, V. I.; Caulton, K. G.; Clot, E.; Eckert, J.; Eisenstein, O.; Gusev, D. G.; Grushin, V. V.; Hauger, B. E.; Klooster, W.; Koetzle, T. F.; McMullan, R. K.; O'Loughlin, T. J.; Pélissier, M.; Ricci, J. S.; Sigalas, M. P.; Vymenits, A. E. *J. Am. Chem. Soc.* **1993**, *115*, 7300.

(6) Empsall, H. D.; Hyde, E. M.; Mentzer, E.; Shaw, B. L. *J. Chem. Soc., Dalton Trans.* **1976**, *20*, 2069.

(7) (a) Werner, H.; Wolf, J.; Höhn, A. *J. Organomet. Chem.* **1985**, *287*, 395. (b) Goldman, A. S.; Halpern, J. *J. Organomet. Chem.* **1990**, *382*, 237.

Here we report the observation of inequivalent hydrides in Ir(H)₂X(P^tBu₂Ph)₂ by ¹H NMR spectroscopy. We will connect this observation to previous theoretical studies and discuss the effect of the halide and phosphine identity on H₂ binding in related systems.

Results and Discussion

Fluxional Behavior of Ir(H)₂X(P^tBu₂R)₂. (a) Decoalescence.

The variable-temperature ¹H NMR spectroscopic study of Ir(H)₂X(P^tBu₂Ph)₂ reveals decoalescence behavior of the hydride signal. For example, in the case of a toluene-*d*₈ solution of Ir(H)₂I(P^tBu₂Ph)₂, this signal is observed as a triplet (²J_{PH} = 13 Hz) at δ -32.2 at room temperature, but it splits into two broad (145 Hz) resonances⁸ at δ -20.1 and -44.4 as the temperature is lowered to -100 °C (Figure 1). The decoalescence temperature is ca. -65 °C, which provides⁹ a free energy of activation of 8.0 kcal/mol for the hydride site exchange at -65 °C. Line shape analysis⁹ of the ¹H NMR spectra recorded between -20 and -95 °C resulted in an Eyring plot (Figure 2) with ΔH[‡] = 7.9 ± 0.2 kcal/mol and ΔS[‡] = 0.1 ± 1.2 eu. This near-zero entropy change is consistent with an intramolecular mechanism, and the triplet structure at 25 °C demonstrates that there is no rupture of the Ir-H or Ir-P bonds during the fluxional process.

The low-temperature limiting hydride chemical shifts are similar to those of other relevant complexes. The hydride chemical shift of IrHCl₂(P^tBu₂Ph)₂, in which the hydride occupies the apical position in a square-pyramidal geometry, is -48.5 ppm.⁶ The hydride chemical shift *trans* to chloride in Ir(H)₂Cl(Cytp) is -22.3 ppm.¹⁰ Therefore, we assign the -44-ppm resonance to a hydride which is pseudo-*trans* to an empty coordination site and the -20-ppm resonance to a hydride which is pseudo-*trans* to the halide ligand. This spectroscopic assignment would also be consistent with the solid-state structure (neutron diffraction) of Ir(H)₂Cl(P^tBu₂Ph)₂ (Figure 3) in which one of the H-Ir-Cl angles is 156° and the other is 131°.⁵

(8) The line width was 35 Hz in CD₂Cl₂ at -100 °C and no evidence was obtained for any large (>30 Hz) proton-proton coupling constants in the low-temperature ¹H NMR spectra of the Ir(H)₂X(P^tBu₂Ph)₂ complexes.

(9) Oki, M. In *Applications of Dynamic NMR Spectroscopy to Organic Chemistry*; VCH Publishers: Deerfield Beach, 1985, Chapter 1.

(10) Yang, C.; Socol, S. M.; Kountz, D. J.; Meek, D. W.; Glaser, R. *Inorg. Chim. Acta* **1986**, *114*, 119.

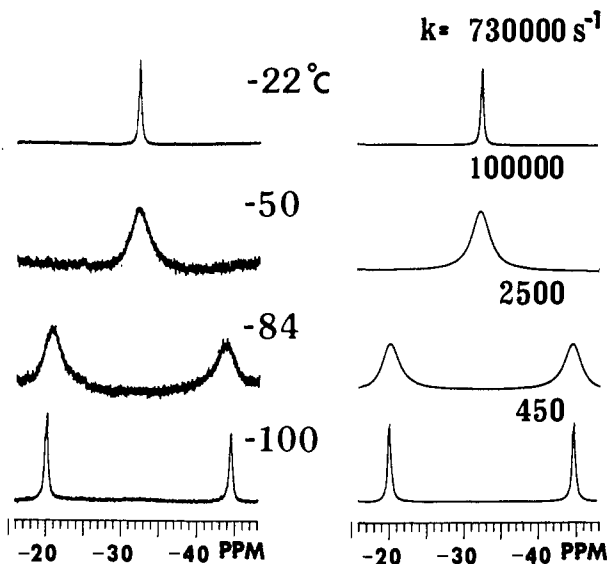


Figure 1. Experimental (left) and calculated (right, with rate constants) ¹H NMR spectra (hydride region only) for Ir(H)₂I(P^tBu₂Ph)₂ in toluene-*d*₈.

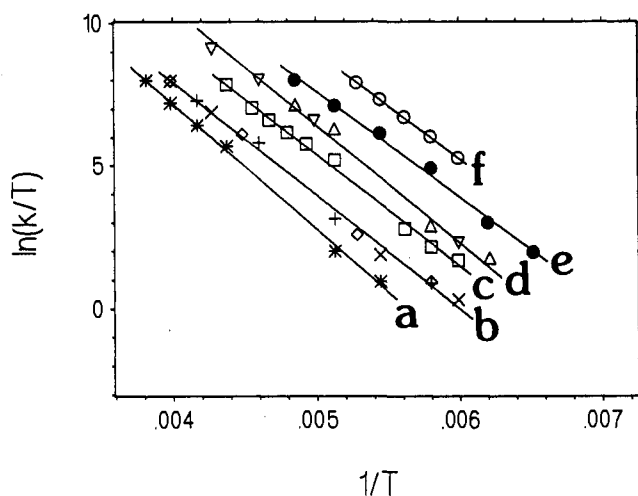


Figure 2. Eyring plots for the rate of hydride site exchange in Ir(H)₂X-(P^tBu₂Ph)₂ for X = I (a, in CD₂Cl₂; b, in toluene-*d*₈), Br (c, in CD₂Cl₂; d, in toluene-*d*₈), and Cl (e, CD₂Cl₂; f, in toluene-*d*₈). Lines b and d include data derived from different concentrations of complex.

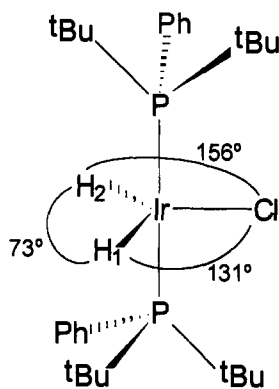


Figure 3. Structure of IrH₂Cl(P^tBu₂Ph)₂.

An *ab initio* study of Ir(H)₂Cl(PH₃)₂ provides an explanation for this distortion.⁵ Although the Y structure (Scheme 1) was calculated to be the energy minimum, distortions of the H–Ir–Cl angles do not require large amounts of energy (<3.3 kcal/mol) if the H–Ir–H angle remains approximately 73°. Thus, pseudo-T-shaped structures are energetically accessible.

Scheme 1

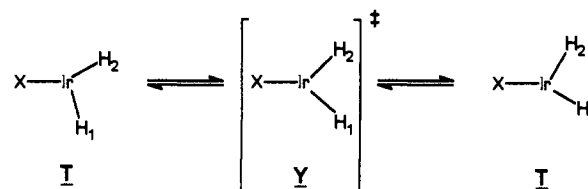


Table 1. *T*₁ (ms) Relaxation Time of the Hydride Ligands in Ir(H)₂X(P^tBu₂Ph)₂ in Toluene-*d*₈

<i>T</i> , K	X		
	Cl	Br	I
282	342	337	353
268	248	244	263
251	181	193	204
234	148	149	147
217	143	135	<i>a</i>
201	198	<i>a</i>	<i>a</i>
184	274	<i>a</i>	240

^a *T*₁ was not determined because of strong broadening of the IrH₂ resonance(s).

The experimental kinetic data for Ir(H)₂I(P^tBu₂Ph)₂ can be rationalized in terms of the site exchange shown in Scheme 1 where a ground state T-shaped structure lies 8 kcal/mol below a transition state of Y geometry. The disparity between the ground-state structure calculated (*ab initio*) for Ir(H)₂Cl(PH₃)₂ and that observed for examples with extremely bulky phosphines must originate in steric repulsion between phosphine substituents and the Ir(H)₂X moiety. Steric interactions of this type were identified in the T-distorted ground-state structure of Ir(H)₂Cl-(P^tBu₂Ph)₂.⁵

(b) Is the H/H Distance Dependent on the Halide Coligand?

A variable-temperature *T*₁ study can be useful for a qualitative comparison of the H–Ir–H distances as the group X is varied in Ir(H)₂X(P^tBu₂Ph)₂. The relaxation rate, 1/*T*₁, for the metal-bound protons is where the contributions are due to the dipole–

$$1/T_1 = 1/T_1(\text{H}\cdots\text{H}) + 1/T_1(\text{H}\cdots\text{H}^*)$$

dipole interactions between the phosphine protons and hydride ligands (1/*T*₁(H...H*)) and between the hydrides themselves (1/*T*₁(H...H)).¹¹ The latter contribution is quite significant in the present case. In Ir(H)₂Cl(P^tBu₂Ph)₂, 1/*T*_{1min} is 7 s⁻¹ at 300 MHz, and from the H...H distance of 1.817 Å (neutron diffraction)⁵ the 1/*T*_{1min}(H...H) contribution of 3.6 s⁻¹ (51% of the observed relaxation rate) can be calculated. It is reasonable to assume¹² a negligible dependence of 1/*T*₁(H...H*) on X and any substantial changes in 1/*T*₁ should be due to the 1/*T*₁(H...H) contribution which is extremely sensitive to H...H distance variations. For example, 1/*T*_{1min}(H...H) = (3.87 × 10⁴)*r*⁻¹*r*(H...H)⁻⁶, where *ν* is the resonance frequency in MHz and *r*(H...H) is the distance in Å.¹¹ Thus, the equation predicts a 32% increase in *T*_{1min} if the H–Ir–H angle increases by 10° assuming the same Ir–H distances: 1.512 and 1.553 Å.

The experimental *T*₁ data for the hydride relaxation in Ir(H)₂X(P^tBu₂Ph)₂ (Table 1) are very similar at comparable temperatures. The observed differences are typically within the error limits of the technique and do not exceed 14%. This observation leads to the conclusion that the distortion of the molecular geometry which is the cause of the inequivalence of the hydrides in Ir(H)₂X(P^tBu₂Ph)₂ does not involve appreciable

(11) Proton–phosphorus dipole–dipole interactions are weak and can be neglected. Desrosiers, P. J.; Cai, L.; Lin, Z.; Richards, R.; Halpern, J. *J. Am. Chem. Soc.* 1991, 113, 3027.

(12) A referee suggests that the constancy of the *T*₁ value down the halides arises from fortuitous compensation of decreasing *T*₁(H...H) and *T*₁(H...H*). We prefer our explanation as simpler.

Table 2. Spectroscopic and Hydride-Site Exchange Activation Parameters for $\text{Ir}(\text{H})_2\text{X}(\text{P}^t\text{Bu}_2\text{Ph})_2$

X	low-temperature $\delta(\text{IrH})$	ΔH^\ddagger	ΔS^\ddagger
Cl	<i>a</i>	7.4 ± 0.2^b	7.7 ± 0.4^b
Cl	$-24.9; -43.1^c$	7.3 ± 0.3^c	4.6 ± 1.5^c
Br	$-23.6; -42.4^b$	8.0 ± 0.2^b	5.6 ± 1.4^b
Br	$-23.1; -44.9^c$	7.8 ± 0.2^c	2.2 ± 0.9^c
I	$-20.1; -44.4^b$	7.9 ± 0.2^b	0.1 ± 1.2^b
I	$-19.8; -45.9^c$	8.7 ± 0.2^c	2.1 ± 0.9^c

^a The decoalescence was not reached in toluene-*d*₈; $\Delta\delta = 15.2$ ppm was assumed, based on comparison to $\text{Ir}(\text{H})_2\text{Br}(\text{P}^t\text{Bu}_2\text{Ph})_2$ in toluene-*d*₈.^b In toluene-*d*₈. ^c In CD_2Cl_2 .

changes in the H...H distance and, thus, the H–Ir–H angle. For the latter, the actual changes should be less than 5° based on the maximum difference in the T_1 values (14%).

(c) Fluxionality for a Smaller Phosphine Analog. In contrast to the above, $\text{Ir}(\text{H})_2\text{X}(\text{P}^i\text{Bu}_2\text{Me})_2$ compounds show only one hydride chemical shift down to -100°C . At the lowest attainable temperature, the broadest line ($\Delta = 80$ Hz, -100°C) was observed for $\text{Ir}(\text{H})_2[\text{P}^i\text{Bu}_2\text{Me}]_2$ in toluene. High viscosity of the solvent is, perhaps, responsible for the line width rather than a fluxional process, since in less viscous CD_2Cl_2 , this resonance was sharp enough to not obscure the proton–phosphorus coupling. For a related compound $\text{Ir}(\text{H})_2\text{Cl}[\text{P}^i\text{Pr}]_2$ the hydrides were found to be equivalent at 77 K by solid-state NMR.¹³ Thus, the absence of the decoalescence behavior for $\text{Ir}(\text{H})_2\text{X}[\text{P}^i\text{Bu}_2\text{Me}]_2$ most probably reflects undistorted Y-shaped structure for this smaller phosphine.

(d) Halide Dependence of the Fluxionality Barrier. The ^1H NMR spectroscopic and kinetic data for the full range of halide complexes $\text{Ir}(\text{H})_2\text{X}(\text{P}^t\text{Bu}_2\text{Ph})_2$ are summarized in Table 2. The rate of intramolecular exchange significantly accelerates in the order $\text{I} < \text{Br} < \text{Cl}$. For example, $k_{\text{Cl}}/k_{\text{I}} = 143$ and $k_{\text{Br}}/k_{\text{I}} = 12$ in toluene at 200 K. Surprisingly, however, the effect is *not enthalpic* in origin. As it is seen from Table 2 and from the nearly-identical slopes in Figure 2, the ΔH^\ddagger values do not depend (significantly) on X, changing only from 7.4 to 8.0 kcal/mol in toluene.

We have expended the effort to look for solvent effects on the site exchange rate. There are two reasons to anticipate only small solvent effects on the activation parameters (Table 2) when comparing CH_2Cl_2 and aromatic solvents. First, the $\text{Ir}(\text{H})_2\text{X}(\text{P}^t\text{Bu}_2\text{R})_2$ molecules are very crowded due to the large phosphines, leaving no site for solvent incorporation. In addition, the hydride motion occurs with very little structural reorganization of the $\text{IrX}(\text{P})_2$ atoms and thus the solvent sheath should be very similar throughout the rearrangement. Indeed, ΔH^\ddagger values show no major changes on comparing the two solvents. Any solvent effect is reflected in the ratio $k(\text{toluene-}d_8)/k(\text{CD}_2\text{Cl}_2)$, which is between 2.9 and 3.8 for $\text{Ir}(\text{H})_2\text{X}(\text{P}^t\text{Bu}_2\text{Ph})_2$ at 200 K.¹⁴

Significantly positive ΔS^\ddagger values of 7.7 ± 0.4 and 5.6 ± 1.4 eu found for the hydride exchange in $\text{Ir}(\text{H})_2\text{Cl}(\text{P}^t\text{Bu}_2\text{Ph})_2$ and $\text{Ir}(\text{H})_2\text{Br}(\text{P}^t\text{Bu}_2\text{Ph})_2$, respectively, seem at first glance to be inconsistent with an intramolecular process. At the same time, they are inconsistent with a bimolecular process, where a substantially negative ΔS^\ddagger is expected. In general, it is unreasonable to suspect that different site exchange mechanisms can operate in $\text{Ir}(\text{H})_2\text{X}(\text{P}^t\text{Bu}_2\text{Ph})_2$ depending on the halide identity. Experiments with different concentrations of the complexes

(13) Wishniewski, L. L.; Mediati, M.; Jensen, C. M.; Zilm, K. W. *J. Am. Chem. Soc.* **1993**, *115*, 7533.

(14) (a) There is currently an inability of physical theories to account quantitatively for solvent effects on rates. A decrease in reaction rate upon increasing solvent polarity is commonly associated^{14b,c} with a transition state of lower polarity than the ground state. Ground-state stabilization by the more coordinating solvent (CD_2Cl_2 vs toluene-*d*₈) can be an alternative explanation to purely polarity-based considerations. (b) Reichardt, C. *Solvents and Solvent Effects in Organic Chemistry*; VCH Publishers: New York, 1988, Chapter 5. (c) Connors, K. A. *Chemical Kinetics: The Study of Reaction Rates in Solution*; VCH Publishers: New York, 1990.

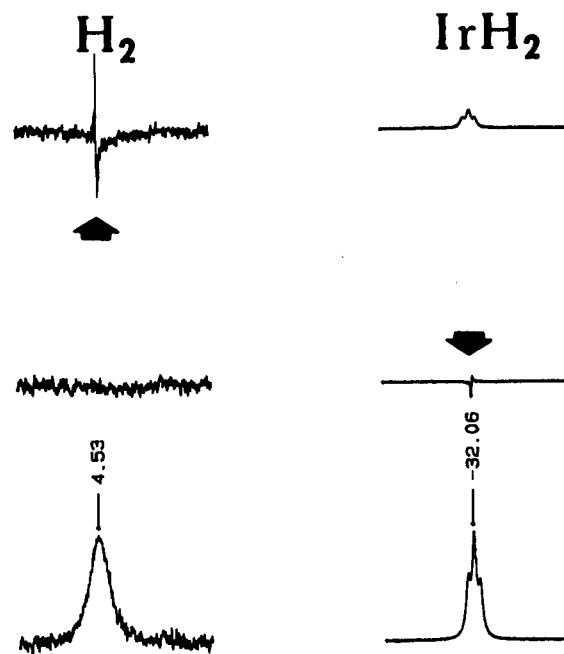


Figure 4. Effects of saturation transfer in ^1H NMR spectra (free H_2 and hydride regions) of $\text{Ir}(\text{H})_2\text{Cl}(\text{P}^t\text{Bu}_2\text{Ph})_2$ under 700 Torr of H_2 in toluene-*d*₈ at -5°C . Saturation was applied at the indicated positions or, in the case of the reference (bottom) spectrum, between the resonances. All spectra were measured and plotted under otherwise identical conditions.

(Figure 2, X = Br, I) show no concentration dependence, strongly supporting the intramolecular character of the exchange. We believe that quantum-mechanical tunneling of the hydride ligands can operate, to a varying degree, in all $\text{Ir}(\text{H})_2\text{X}(\text{PR}_3)_2$ complexes, precluding correct determination of the ΔS^\ddagger values.^{15,16}

H_2 Binding to $\text{Ir}(\text{H})_2\text{X}(\text{P}^t\text{Bu}_2\text{Ph})_2$ (X = Cl, Br, I). The extreme steric bulk of $\text{P}^t\text{Bu}_2\text{Ph}$ strongly disfavors H_2 binding by these molecules. For each halide, spectroscopic evidence supports equilibrium 1, but lying very far to the left. At room temperature, the ^1H NMR of all $\text{Ir}(\text{H})_2\text{X}(\text{P}^t\text{Bu}_2\text{Ph})_2$ molecules under H_2 show broadened resonances of dissolved hydrogen ($\Delta = 56\text{--}62$ Hz) at δ 4.5 and that of $\text{Ir}(\text{H})_2$ ($\Delta = 40\text{--}46$ Hz) at ca. δ -32 . Above -20°C , the T_1 relaxation measurements give identical T_1 values for dissolved hydrogen and for the hydrides. The T_1 values for the H_2 signals (200–300 ms at -10°C) are appreciably shorter than those of free H_2 in the absence of the metal complex (>1 s). Only at temperatures below -20°C are the relaxation times for dissolved H_2 increased because of slowing the rate of equilibrium 1 on the relaxation time scale. The most convincing evidence for the existence of equilibrium 1 is obtained by a spin saturation-transfer experiment for $\text{Ir}(\text{H})_2\text{Br}(\text{P}^t\text{Bu}_2\text{Ph})_2$. At $+10^\circ\text{C}$, CW decoupling at δ 4.5 effectively saturates the $\text{Ir}(\text{H})_2$ peak at δ -32.7 and vice versa. This clearly shows that protons of the dihydride complex and H_2 are exchanging quickly in the unobserved fluxional $\text{Ir}(\text{H})_2\text{Br}(\text{H}_2)(\text{P}^t\text{Bu}_2\text{Ph})_2$. Figure 4 shows this behavior for the chloride complex. In all cases, in the temperature range 20 to -90°C , no detectable amount of $\text{Ir}(\text{H})_2\text{X}(\text{H}_2)(\text{P}^t\text{Bu}_2\text{Ph})_2$ is directly observed by ^1H and $^{31}\text{P}\{^1\text{H}\}$ NMR. While this precludes further kinetic and thermodynamic study, the averaging and shortening of T_1 for free H_2 and for coordinated hydrides represents a phenomenon useful for proving the existence of a hydride/dihydrogen compound when direct

(15) Bell, R. P. In *The Tunnel Effect in Chemistry*, Chapman and Hall: London and New York, 1980, Chapter 3.

(16) We attempted to slow any quantum tunnelling contribution by replacement of H by deuterons. The ^2H NMR spectrum of $\text{Ir}(\text{D})_2\text{Cl}(\text{P}^t\text{Bu}_2\text{Ph})_2$ shows no decoalescence at -102°C in CH_2Cl_2 . Since the resonance frequency is reduced by a factor of 6.5 compared to the protio compound, this factor overwhelms any change in site exchange rate and thus leaves the experiment inconclusive.

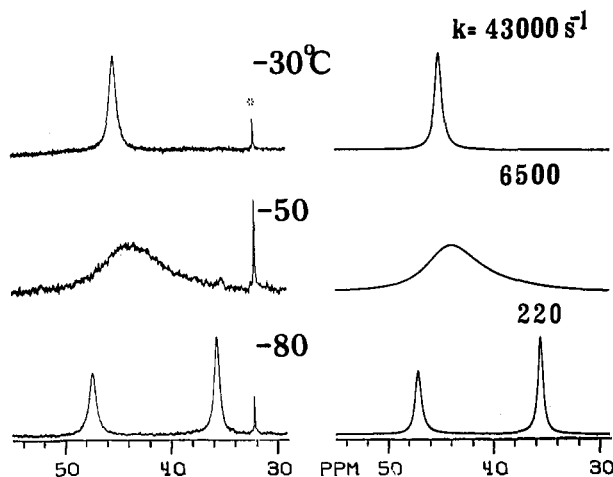


Figure 5. Observed (left) and calculated (right, with rate constants for H₂ loss from Ir(H)₂Cl(H₂)(P^tBu₂Me)₂) variable-temperature ³¹P{¹H} NMR spectra of Ir(H)₂Cl(H₂)(P^tBu₂Me)₂ under 700 mm of H₂ in toluene-*d*₈. The resonance of Ir(H)₂Cl(H₂)(P^tBu₂Me)₂ appears at 35.5 ppm. The asterisk indicates an inert impurity at 32 ppm.

observation is not possible (e.g., when the equilibrium population is low).

Kinetics of H₂ Binding to Ir(H)₂X(P^tBu₂Me)₂ (X = Cl, Br, I). Below 20 °C, variable-temperature ¹H and ³¹P{¹H} NMR study demonstrates appreciable H₂ binding by all of these halide compounds, consistent with the smaller size of P^tBu₂Me (i.e., dominant steric effect).¹⁷ A significant steric influence on the extent of H₂ binding has been demonstrated previously in Ir(H)₂-Cl(PR₃)₂ systems.^{3b} Rate data for loss of H₂ from Ir(H)₂X-(H₂)(P^tBu₂Me)₂ obtained by fitting the experimental variable-temperature ³¹P{¹H} NMR spectra (see, for example, Figure 5) using the simulation program DNMR5 are displayed in an Eyring plot in Figure 6. Data obtained for the dissociation of D₂ from Ir(D)₂(D₂)Cl(P^tBu₂Me)₂ are also compared to those for loss of H₂ from Ir(H)₂(H₂)Cl(P^tBu₂Me)₂ in an Eyring plot in Figure 6. Activation parameters obtained by linear least-squares fitting of the data are shown in Table 3.

The ΔS[‡] values are all positive but of small magnitude consistent with a process with only slightly increased degrees of freedom in the transition state as a result of the departing H₂ molecule. The values show that the transition state is reached with only a small amount of bond breaking. Perhaps the higher entropy of D₂ vs H₂ is reflected in a higher ΔS[‡] for Ir(D)₂Cl(D₂)(P^tBu₂Me)₂ than for Ir(H)₂Cl(H₂)(P^tBu₂Me)₂. Unfortunately, the relatively large error makes further quantitative comparisons impossible. The compounds Ir(H)₂X(H₂)(P^tBu₂Me)₂ are among the most unstable known dihydrogen complexes and the ΔH[‡] values listed in Table 3 are at the lower limit of values found for the loss of H₂. Comparable activation parameters of 8.8 ± 0.1 and 12.1 ± 1.0 kcal/mol were reported for [Ru(H₂)(H)₃(PPh₃)₃]⁺ and Cr(H₂)(CO)₃(PCy₃)₂, respectively.^{2b,18} In the case of the kinetically more stable W(H₂)(CO)₃(PCy₃)₂ and Ru(H₂)(H)₂(PPh₃)₃, ΔH[‡] values are noticeably higher: 16.9 ± 2.2 and 17.9 ± 0.2 kcal/mol, respectively.^{2c,14} Unfortunately, meaningful comparison of the activation entropies is practically impossible because of the large error (several cal mol⁻¹ K⁻¹) in the ΔS[‡] data available in the literature. The error, perhaps, is mainly responsible for the strongly different values reported for [Ru(H₂)(H)₃(PPh₃)₃]⁺ (-12 eu), Cr(H₂)(CO)₃(PCy₃)₂ (-2.1 eu), W(H₂)(CO)₃(PCy₃)₂ (+10.4 eu), and Ru(H₂)(H)₂(PPh₃)₃ (+3 eu).^{2b,c,15}

(17) It is not possible that the P^tBu₂Ph analog binds H₂ poorly due to a phenyl *o*-hydrogen interaction because the neutron diffraction structure⁵ shows these to be absent. Also, the -44 ppm hydride chemical shift is diagnostic of hydride *trans* to an empty coordination site.

(18) Halpern, J.; Cai, L. S.; Desrosiers, P. J.; Lin, Z. R. *J. Chem. Soc., Dalton Trans.* 1991, 717.

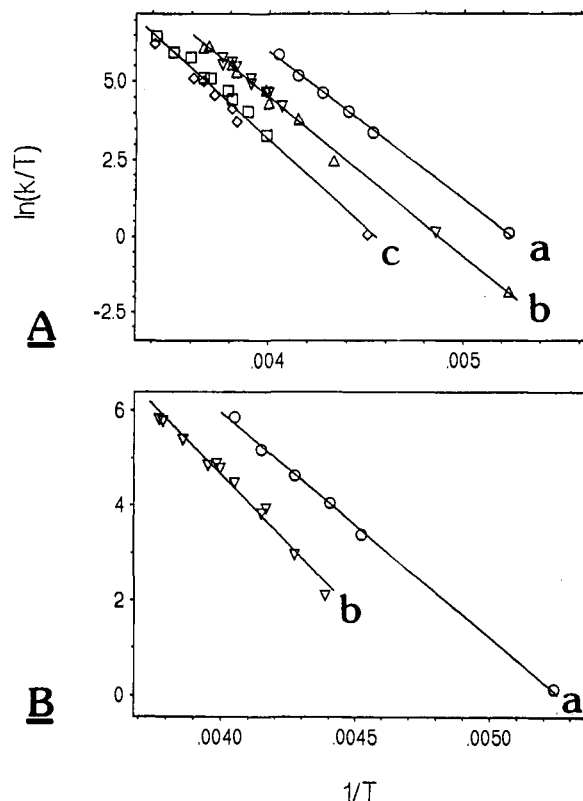


Figure 6. (A) Eyring plot of rate data for H₂ loss from Ir(H)₂X(H₂)(P^tBu₂Me)₂ for chloride (a), bromide (b), and iodide (c). Lines b and c contain data for two different concentrations of complex (identified by different symbols) and show the concentration independence of *k*. (B) Eyring plots for dissociation of D₂ from Ir(D)₂(D₂)Cl(P^tBu₂Me)₂ (b) and H₂ from Ir(H)₂Cl(H₂)(P^tBu₂Me)₂ (a).

Table 3. Kinetic and Thermodynamic Data for H₂ and D₂ Loss from Ir(H)₂(H₂)X(P^tBu₂Me)₂ (X = Cl, Br, I) and Ir(D)₂(D₂)Cl(P^tBu₂Me)₂ in Toluene-*d*₈

	<i>M</i> (×10 ⁻²)	ΔH [‡] , kcal/mol	ΔS [‡] , eu	ΔH [‡] , kcal/mol	ΔS [‡] , eu
Cl	41	9.4 ± 0.2	2.3 ± 0.9	6.8 ± 0.2	19.2 ± 0.7
Br	29	10.2 ± 0.2	2.4 ± 1.0	7.9 ± 0.9 ^a	19.7 ± 3.2 ^a
	47	10.1 ± 0.2	2.4 ± 0.9		
I	22	10.8 ± 0.5	2.8 ± 2.0	9.3 ± 0.2 ^a	22.7 ± 0.8 ^a
	35	11.3 ± 0.3	3.7 ± 1.1		
Cl ^b	28	11.7 ± 0.5 ^a	8.7 ± 2.2 ^a	-	-
	41			7.7 ± 0.5	20.7 ± 1.8

^a Parameters were determined combining the data at two concentrations when less than five data points were measured for one concentration.

^b Data for Ir(D)₂Cl(D₂)(P^tBu₂Me)₂.

As could be expected for a process involving bond rupture, the kinetic isotope effect found for the D₂ loss from Ir(D)₂(D₂)Cl(P^tBu₂Me)₂ is relatively high; *k*_H/*k*_D are 1.8 and 6 at 20 °C and -50 °C, for example. These values are within the range of *k*_H/*k*_D for W(H₂)(CO)₃(PCy₃)₂, Cr(H₂)(CO)₅, and IrHCl₂(H₂)(PCy₃)₂: 1.7 (25 °C), 5 (room temperature) and 6-7 (-60 to -70 °C), respectively.^{2c,4,19}

ΔH[‡] values increase in the order Cl < Br < I. The dissociative transition state could be expected to show the opposite trend based purely on size of the halide, with the larger iodide²⁰ promoting a decrease in coordination number. Therefore, the data indicate that electronic factors dominate steric considerations. We suggest a transition state in which a halide lone pair interacts

(19) Church, S. P.; Grevels, F.-W.; Hermann, H.; Schaffner, K. *J. Chem. Soc., Chem. Commun.* 1985, 30.

(20) Tolman, C. A. *Chem. Rev.* 1977, 77, 313.

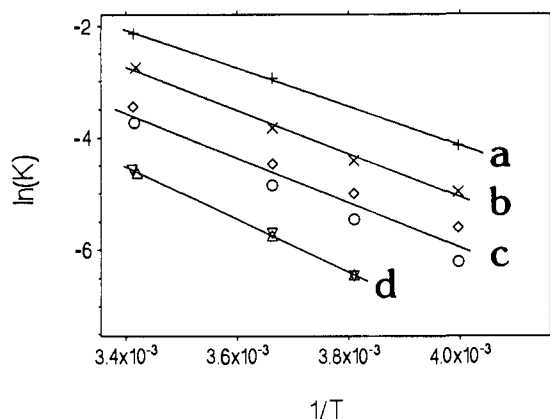


Figure 7. Equilibrium constants for H_2 dissociation from $\text{Ir}(\text{H})_2\text{X}(\text{H}_2)(\text{P}^t\text{Bu}_2\text{Me})_2$ displayed as $\ln K$ vs $1/T$. Lines a, c, and d are for I, Br, and Cl, respectively. Line b is for D_2 binding to $\text{Ir}(\text{D})_2\text{Cl}(\text{P}^t\text{Bu}_2\text{Me})_2$. Lines c and d include data collected at two different concentrations of complex.

constructively with the metal center, partially displacing the dihydrogen ligand. The ΔH^\ddagger values contain evidence for the existence of increasing **multiple-bond character** between the iridium metal center and the halide ligands in the transition state with the established²¹ capacity for π -bonding ($\text{Cl} > \text{Br} > \text{I}$) determining the trend.

Thermodynamics of H_2 Loss from $\text{Ir}(\text{H})_2\text{X}(\text{P}^t\text{Bu}_2\text{Me})_2$ ($\text{X} = \text{Cl}, \text{Br}, \text{I}$). The π -donation invoked to explain the trends in ΔH^\ddagger should also influence the thermodynamics of H_2 binding to $\text{Ir}(\text{H})_2\text{X}(\text{P}^t\text{Bu}_2\text{Me})_2$ complexes. Thermodynamic data were obtained at temperatures above -30°C due to the slow rate of H_2 transport into and out of toluene in an NMR tube at temperatures below -30°C . Data obtained for dissociation of $\text{Ir}(\text{H})_2(\text{H})_2\text{X}(\text{P}^t\text{Bu}_2\text{Me})_2$ are displayed in a plot of $\ln K$ vs $1/T$ in Figure 7.

Values obtained by linear least-squares fitting of the data are contained in Table 3. The ΔS° values are large and positive, as expected for a dissociative reaction. The magnitude of ΔS° also compares well with previously obtained values: 23.2 ± 1 , 23.8 ± 2.1 , and 25.6 ± 1.7 eu for $\text{Ru}(\text{H}_2)\text{HCl}(\text{CO})(\text{P}^i\text{Pr}_3)_2$,²² $\text{Mo}(\text{H}_2)(\text{CO})_3(\text{PCy}_3)_2$,^{2a} and $\text{Cr}(\text{H}_2)(\text{CO})_3(\text{PCy}_3)_2$,^{2b} respectively. These same complexes, having been characterized by ΔH° of 7.7 ± 0.2 , 6.5 ± 0.2 , and 7.3 ± 0.1 kcal/mol, respectively, have thermodynamic stability similar to that of $\text{Ir}(\text{H})_2\text{Cl}(\text{H}_2)(\text{P}^t\text{Bu}_2\text{Me})_2$. The adduct is enthalpically favored for all halides. The magnitude of the ΔH° values show the same trend as the ΔH^\ddagger values: $\text{Cl} < \text{Br} < \text{I}$.

Investigation of the D_2 addition to $\text{Ir}(\text{D})_2\text{Cl}(\text{P}^t\text{Bu}_2\text{Me})_2$ reveals an equilibrium isotope effect, $K_D/K_H = 2.7$ at 260 K. At this temperature, the ratio is 2 for the only other case of $\text{H}_2(\text{D}_2)$ coordination, $\text{IrHCl}_2(\text{PCy}_3)_2 + \text{H}_2(\text{D}_2)$, where the isotope effect has been measured so far.⁴ A similar effect with $K_D/K_H = 1.9$ (260 K) was found for an oxidative addition of $\text{H}_2(\text{D}_2)$ to $\text{WI}_2(\text{PMe}_3)_4$, where the W–D bonds in the product were shown to be *ca.* 1.8 kcal/mol stronger than the W–H bonds.²³ The last available example is $\text{Cp}_2\text{Ta}(\mu\text{-CX}_2)_2\text{Ir}(\text{CO})(\text{PPh}_3)$, where for the oxidative addition of H_2 ($\text{X} = \text{H}$) and D_2 ($\text{X} = \text{D}$), $K_D/K_H = 2.3$ (260 K).²⁴ It is interesting to note that in these cases the isotope effects are enthalpic in origin: $\Delta H^\circ(\text{D}) - \Delta H^\circ(\text{H}) = 0.9 \pm 0.7$ ($\text{Ir}(\text{H})_2\text{Cl}(\text{P}^t\text{Bu}_2\text{Me})_2$), 1.9 ± 1.3 ($\text{WI}_2(\text{PMe}_3)_4$), 1.0 ± 0.6 kcal/mol ($\text{Cp}_2\text{Ta}(\mu\text{-CX}_2)_2\text{Ir}(\text{CO})(\text{PPh}_3)$). Both M–D and M–(D_2) bonds seem to be substantially stronger than the corresponding M–H or M–(H_2) bonds.

In general, a great thermodynamic difference between the reactions of dihydrogen coordination or oxidative addition should not be expected. A higher enthalpy change can, perhaps, be associated with the latter reaction. The few entropy unit change found for the equilibria $\text{M}(\text{H}_2)\text{L}_n \rightleftharpoons \text{M}(\text{H})_2\text{L}_n$ clearly shows that the intramolecular part of an oxidative addition of H_2 is not significantly "entropy consuming".¹ Thus, ΔS° should be mainly determined by the loss of the rotational freedom of H_2 on "adduct" formation. The "adduct" can be a stable dihydrogen complex or a transition state if further (oxidative) reaction occurs. Unfortunately, the existing literature data are too limited to argue either for or against these considerations. If for the oxidative addition of H_2 to $\text{Cp}_2\text{Ta}(\mu\text{-CH}_2)_2\text{Ir}(\text{CO})(\text{PPh}_3)$ the ΔS° of -23.7 ± 0.6 eu is "reasonable", the example with $\text{WI}_2(\text{PMe}_3)_4$ gave a very large ΔS° of -45 ± 2 eu.^{23,24}

Reactivity of H_2 with $\text{IrH}_2\text{F}(\text{P}^t\text{Bu}_2\text{R})_2$ ($\text{R} = \text{Me}$). We have shown²⁵ that late transition metal fluorides are often quite different from Cl, Br, and I in their binding and also in their reactivity. For example, $\text{RuHF}(\text{CO})(\text{P}^t\text{Bu}_2\text{Me})_2$ reacts with H_2 to eliminate HF whereas this behavior was not observed for the other halides. We were therefore interested in obtaining kinetic and thermodynamic information on H_2 binding to iridium dihydride fluorides. Unfortunately, $\text{IrH}_2\text{F}(\text{P}^t\text{Bu}_2\text{Ph})_2$ reacts in an analogous fashion to the ruthenium fluoride mentioned above producing $\text{IrH}_5(\text{P}^t\text{Bu}_2\text{Ph})_2$ (³¹P and ¹H NMR evidence) and HF (through observation of glass etching), precluding further study. The common reactivity for these different compounds underscores the high Brønsted basicity of fluoride in the presumed dihydrogen complexes $\text{RuHF}(\text{H}_2)(\text{CO})(\text{P}^t\text{Bu}_2\text{Me})$ and $\text{Ir}(\text{H})_2\text{F}(\text{H}_2)(\text{P}^t\text{Bu}_2\text{Ph})_2$. It is also worth highlighting the low acidity of HF under these conditions as evidenced by the lack of significant back reaction between IrH_3L_2 and HF.

Conclusion

The data obtained here are best represented graphically. In Figure 8 reaction coordinate profiles of all of the compounds measured are superimposed with the transition state enthalpy fixed at the same energy for the purpose of comparing ΔH^\ddagger values. The ordering of halides is reversed in the five- and the six-coordinate sides precisely because what *assists* during *dissociation* of H_2 ($\text{X} \rightarrow \text{Ir}$ π -donation) *inhibits binding* of H_2 (or any Lewis base). The magnitude of this effect upon H_2 addition is modest (<0.9 kcal/mol difference from iodide to chloride). The magnitude of the effect upon H_2 dissociation is larger (1.6 kcal/mol). This correlates with the fact that X-ligand lone pairs do not simply stabilize the H_2 -loss transition state, but they *destabilize* the H_2 adduct ground state, by filled/filled repulsions with the filled d_π iridium orbitals. Since the transition state has been established as "tight" (still rigid by the ΔS^\ddagger criterion), such ground-state destabilization should significantly augment the transition state stabilization. Finally, while these π -effects are systematically detectable in our data, their subtle magnitude is evident in the fact that the change to D from H exceeds the change from one halide to another.

The same conclusion has been articulated²⁶ concerning the X-dependence of the thermodynamics of H_2 addition to $\text{IrX}(\text{CO})(\text{PH}_3)_2$: π -donation by X dominates over σ -effects, and increased π -donation makes H_2 addition less exothermic. Paradoxically, criteria of electron density at Ir such as $\nu(\text{CO})$ and oxidation potentials *fail* to correlate these ΔH° trends.

The small size of ΔS^\ddagger for a dissociative process leads to the surprising conclusion that the transition state has little increase in degrees of freedom. That ΔS^\ddagger is only 10% of ΔS° indicates that most of the degrees of freedom remain to be gained along

(21) Poulton, J. T.; Folting, K.; Streib, W. E.; Caulton, K. G. *Inorg. Chem.* **1992**, *31*, 3190.

(22) Gusev, D. G.; Vymenits, A. B.; Bakhmutov, V. I. *Inorg. Chem.* **1992**, *31*, 1.

(23) Rabinovich, D.; Parkin, G. *J. Am. Chem. Soc.* **1993**, *115*, 353.

(24) Hostetler, M. J.; Bergman, R. G. *J. Am. Chem. Soc.* **1992**, *114*, 7629.

(25) Poulton, J. T.; Sigalas, M. P.; Eisenstein, O.; Caulton, K. G. *Inorg. Chem.*, submitted for publication.

(26) Abu-Hasanayn, F.; Krogh-Jespersen, K.; Goldman, A. S. *Inorg. Chem.* **1993**, *32*, 495.

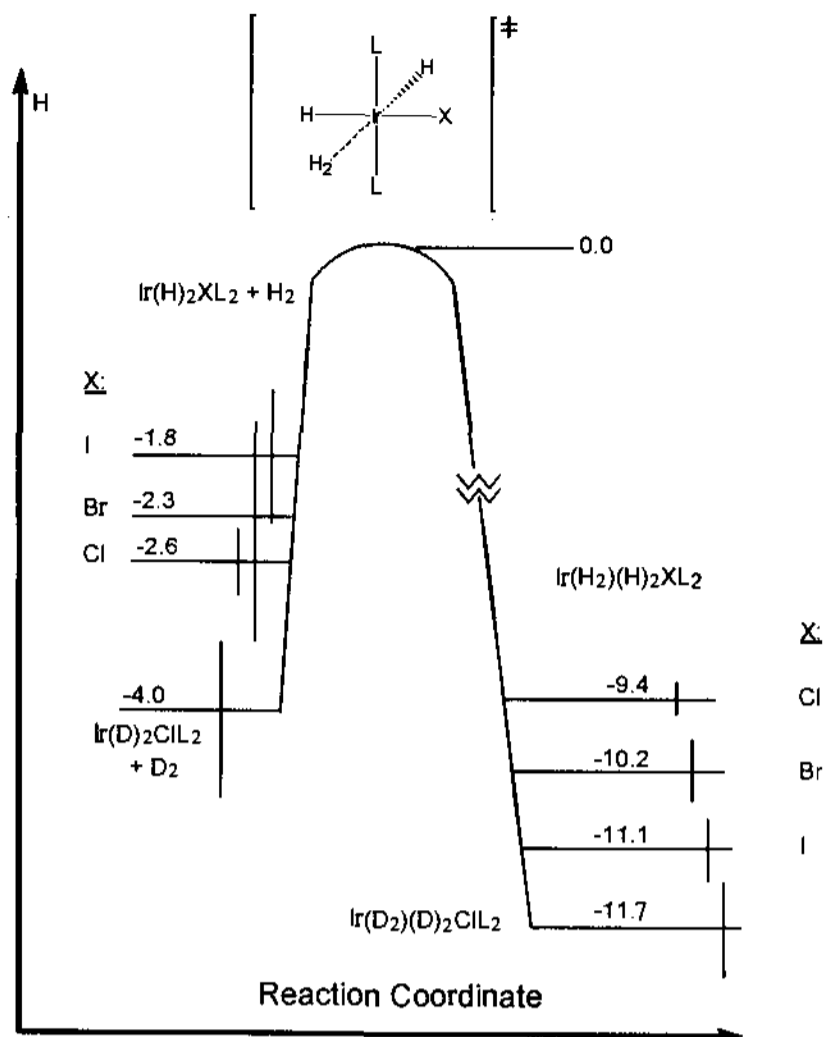
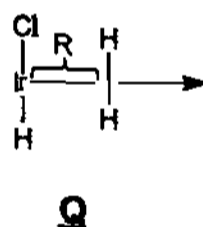
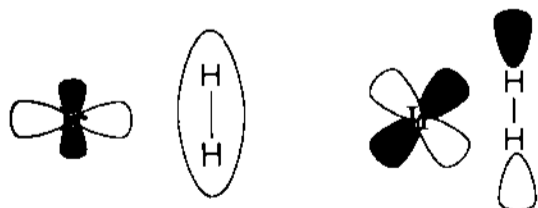


Figure 8. Reaction profile (enthalpies of reaction, kcal/mol, in toluene, with error bars shown to scale) for the reaction $\text{Ir}(\text{H})_2\text{X}(\text{P}^t\text{Bu}_2\text{Me})_2 + \text{H}_2 \rightleftharpoons \text{Ir}(\text{H})_2\text{X}(\text{H})_2(\text{P}^t\text{Bu}_2\text{Me})_2$. Errors accumulate in ΔH^\ddagger for H₂ binding since they are derived by subtraction of ΔH^\ddagger (dissociation) and ΔH° .

the reaction coordinate after the free energy turns downward again. The reaction coordinate is anticipated to be with H₂ perpendicular to, but along the vector shown in **Q**. We propose

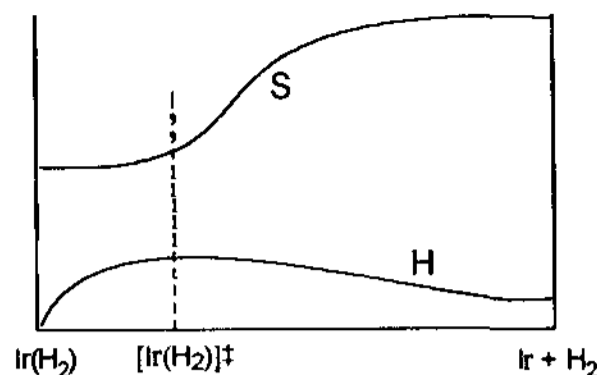


that the free energy turns down at a relatively short distance *R* as a consequence of the character of the M-(H₂) bond. The π back bonding from Ir to H₂ falls off more quickly with distance than it does in a typical σ bond because of the side-to-side character of the overlap. Peculiar to H₂ is the fact that H₂ \rightarrow Ir σ bonding does not involve a directed ligand lone pair, but instead the filled $\sigma(\text{H}-\text{H})$ orbital, whose density is directed perpendicular to the Ir-(H₂ center-of-mass). Its overlap with a metal orbital will



thus decrease more rapidly with distance than if this ligand were PH₃ or NH₃. As a result, along the reaction coordinate (increased *R*), enthalpy will immediately rise but entropy will rise only for larger values of *R*.²⁷

(27) After completion of this manuscript, relevant work has appeared on the activation parameters for H₂ loss from $\text{Ir}(\text{H})_2\text{X}(\text{H})_2(\text{P}^t\text{Pr}_3)_2$ where X = Cl, Br, and I. Le-Husebo, T.; Jensen, C. M. *Inorg. Chem.* 1993, 32, 3797. The halide dependence of ΔG^\ddagger is comparable to that reported here, although their interpretation of the cause is different.



Experimental Section

General. All manipulations were carried out using standard Schlenk and glovebox techniques under prepurified argon. Toluene-*d*₈ was dried over sodium metal and vacuum distilled prior to use. CD₂Cl₂ was dried over CaCl₂ and distilled before use. H₂ (Air Products, Ultra High Purity Grade) and D₂ (Matheson) were used without further purification. All gas transfers were performed on a calibrated gas manifold.

³¹P{¹H} and ¹⁹F NMR spectra were recorded on a Nicolet NT360 spectrometer at 146.2 and 339.7 MHz, respectively. ¹H NMR spectra were recorded on a Varian XL300 spectrometer at 299.9 MHz. Positive ³¹P NMR chemical shifts are downfield from the external 85% H₃PO₄ reference. The standard inversion recovery sequence 180- τ -90 was used to determine *T*₁. All temperatures were carefully calibrated by using the ¹H NMR chemical shifts of methanol. Negative ¹⁹F NMR chemical shifts are upfield from external CFCI₃. Ir(H)₂Cl(P^tBu₂Ph)₂, Ir(H)₂I(P^tBu₂Ph)₂, and Ir(H)₂Cl(P^tBu₂Me)₂ have all been prepared previously.⁶ Ir(H)₂Br(P^tBu₂Ph)₂ and Ir(H)₂Br(P^tBu₂Me)₂ were prepared by stirring the respective chlorides with NaBr in toluene overnight and filtering. Ir(H)₂I(P^tBu₂Me)₂ was prepared by stirring Ir(H)₂Cl(P^tBu₂Me)₂ with NaI in toluene overnight and filtering. Yields for all halide exchanges were essentially quantitative.

Synthesis of Ir(H)₂F(P^tBu₂Ph)₂. A solution of Ir(H)₂Br(P^tBu₂Ph)₂ in benzene was mixed with CsF and stirred overnight. Little conversion was observed by ³¹P{¹H} NMR assay. 18-Crown-6 was then added to the solution which was then stirred overnight. Nearly complete²⁸ conversion to Ir(H)₂F(P^tBu₂Ph)₂ is observed. ³¹P{¹H} NMR in C₆D₆: 61.7 (s). ¹H NMR in C₆D₆: 1.49 (vt, 12 Hz), -32.0 (dt, ²J_{FH} = 46 Hz, ²J_{PH} = 12 Hz). ¹⁹F NMR in C₆D₆: -204 (t, ²J_{FH} = 46 Hz).

Reactivity of Ir(H)₂F(P^tBu₂Ph)₂ with H₂. An NMR tube containing a C₆D₆ solution of Ir(H)₂F(P^tBu₂Ph)₂ was freeze-pump-thaw degassed three times. The head space of the tube was filled with 700 Torr of H₂ gas. The tube was then sealed with a flame. Within 15 min, the only observable product by ³¹P{¹H} NMR was Ir(H)₅(P^tBu₂Ph)₂. The glass of the tube became etched over time, indicating the production of HF.

Sample Preparation. All samples were prepared by transfer of a weighed amount of the solid organometallic compound into an NMR tube. Toluene-*d*₈ (500 μ L) was then added by syringe, and the tube was connected to a gas adapter via Tygon tubing. The solvent was freeze-pump-thaw degassed five times. H₂ (or D₂) gas (700 Torr) was allowed to fill the space above the frozen toluene solution. The gas adapter was then closed and the majority of the tube was immersed in liquid nitrogen. The tube was then sealed with a torch and stored at -15 $^\circ$ C prior to study.

Kinetic Modeling. Between 25 and -90 $^\circ$ C, ³¹P{¹H} NMR spectra (Figure 5) of an equilibrium mixture of Ir(H)₂X(H)₂(P^tBu₂Me)₂ and Ir(H)₂X(P^tBu₂Me)₂ show variable-temperature behavior characteristic of a two-site exchanging system.⁹ Two sharp resonances can be observed at -90 $^\circ$ C, but on raising the temperature, they broaden and coalesce, and the resulting averaged signal finally sharpens. In the case of a true two-site exchange (eq 2), the lifetimes of sites τ_A and τ_B can be expressed

$$\text{A} \xrightleftharpoons[k_{-1}]{k_1} \text{B} \quad (2)$$

using the rate constant *k*₁: $\tau_A = 1/k_1$ and $\tau_B = 1/k_{-1} = R/k_1$ where *R* is the ratio [B]/[A], i.e., the equilibrium constant.⁹ It can be easily shown that for an equilibrium between Ir(H)₂X(H)₂(P^tBu₂Me)₂ (A) and Ir(H)₂X(P^tBu₂Me)₂ (B) (eq 3), the same definitions for the lifetimes, $\tau_A = 1/k_1$ and $\tau_B = R/k_1$ (*R* = [B]/[A]), are valid and can be obtained using the following conventional formulae: $\tau_B = (k_1[\text{H}_2])^{-1}$ and $K = [\text{B}][\text{H}_2]/[\text{A}] = k_1/k_{-1}$. Thus, equilibria 2 and 3 are spectroscopically

(28) Attempts to use this method to synthesize Ir(H)₂F(P^tBu₂Me)₂ failed.

Table 4. NMR Data (in C₆D₆, 25 °C)

	$\delta(^{31}\text{P})$	$\delta(^1\text{H}, ^t\text{Bu})$	$\delta(^1\text{H}, \text{Me})$	$\delta(^1\text{H}, \text{IrH})$
Ir(H) ₂ Br(P ^t Bu ₂ Me) ₂	48 (s)	1.16 (vt, 12 Hz)	1.65 (br s)	-32.7 (t, 12 Hz)
Ir(H) ₂ I(P ^t Bu ₂ Me) ₂	48 (s)	1.12 (vt, 13 Hz)	1.97 (br s)	-32.5 (t, 14 Hz)
Ir(H) ₂ (H ₂)Cl(P ^t Bu ₂ Me) ₂ ^a	35.5 (br s)	c	c	-10.8 (br s)
Ir(H) ₂ (H ₂)Br(P ^t Bu ₂ Me) ₂ ^a	33 (s)	c	c	-10.8 (br s)
Ir(H) ₂ (H ₂)I(P ^t Bu ₂ Me) ₂ ^a	29 (s)	c	c	-10.7 (br s)
Ir(H) ₂ Cl(P ^t Bu ₂ Ph) ₂ ^b	67 (s)	1.43 (vt, 13 Hz)		-32.1 (t, 14 Hz)
Ir(H) ₂ Br(P ^t Bu ₂ Ph) ₂ ^b	68 (s)	1.41 (vt, 13 Hz)		-32.7 (t, 13 Hz)
Ir(H) ₂ I(P ^t Bu ₂ Ph) ₂ ^b	70 (s)	1.39 (vt, 13 Hz)		-32.2 (br t, 13 Hz)

^a -80 °C, in toluene-*d*₈. ^b Phenyl resonances fall within the range 8.15–7.02 ppm. ^c Not determined due to coalescence with the five-coordinate complex.



identical in ³¹P{¹H} NMR and the two parameters, *R* and *k*₁, are sufficient to characterize and simulate the variable-temperature ³¹P{¹H} NMR spectra.²⁹

The [B]/[A] ratio (*R*) can be determined experimentally. To avoid the difficulties with integration of strongly broadened lines, we preferred the determination of *R* at temperatures above the coalescence point, where

$$\delta = a\delta_A + b\delta_B$$

$$a + b = 1$$

δ is the chemical shift of the exchange-averaged resonances, and *a* and *b* are the mole fractions of Ir(H)₂X(H₂)(P^tBu₂Me)₂ and Ir(H)₂X(P^tBu₂Me)₂, respectively.

Care was taken to assure that the chemical shift and peak width at half-height of the ³¹P{¹H} NMR signals were constant over the time of one spectrum acquisition (5–10 min). Peak widths at half-height and chemical shifts for broadened signals were conveniently obtained by use

of a curve-fitting program from the Nicolet software. In each case, a small (<5%) sharp impurity peak believed to be an iridium carbonyl compound was used as an internal reference (Figure 5). The origin of this compound is unknown. Complete line shape analysis of the variable-temperature ³¹P{¹H} NMR spectra was done using DNMR5 (QCMF 059) available from the QCPE at Indiana University.

Thermodynamic Determinations. Transport of H₂ (or D₂) into and/or out of solution proved to be slow at temperatures below -30 °C. Therefore, samples were held at the desired temperature for at least 5 h before spectral measurement in order to assure that both H₂ saturation and equilibrium were attained. The literature data³⁰ on hydrogen solubility were used in the calculations of the equilibrium constants.

Acknowledgment. This work was supported by the National Science Foundation. D.G. is a recipient of a fellowship from the U.S. National Academy of Sciences/AID.

(29) This conclusion can be expressed in a qualitative way: the phosphorus nuclei do not "know" what kind of changes in the environment make them resonate at two different frequencies.

(30) Fogg, P. G. T.; Gerrard, W. *Solubility of Gases in Liquids*, John Wiley & Sons: Chichester, 1991.